Positron Production in Multiphoton Light-by-Light Scattering

D. L. Burke, R. C. Field, G. Horton-Smith, J. E. Spencer, and D. Walz

Stanford Linear Accelerator Center, Stanford University, Stanford, California 94309

S. C. Berridge, W. M. Bugg, K. Shmakov, and A. W. Weidemann

Department of Physics and Astronomy, University of Tennessee, Knoxville, Tennessee 37996

C. Bula, K. T. McDonald, and E. J. Prebys

Joseph Henry Laboratories, Princeton University, Princeton, New Jersey 08544

C. Bamber,* S. J. Boege,† T. Koffas, T. Kotseroglou,‡ A. C. Melissinos, D. D. Meyerhofer,§ D. A. Reis, and W. Ragg‖

Department of Physics and Astronomy, University of Rochester, Rochester, New York 14627

A signal of 106 ± 14 positrons above background has been observed in collisions of a low-emittance 46.6 GeV electron beam with terawatt pulses from a Nd:glass laser at 527 nm wavelength in an experiment at the Final Focus Test Beam at SLAC. The positrons are interpreted as arising from a two-step process in which laser photons are backscattered to GeV energies by the electron beam followed by a collision between the high-energy photon and several laser photons to produce an electron-positron pair. These results are the first laboratory evidence for inelastic light-by-light scattering involving only real photons. [S0031-9007(97)04008-8]

The production of an electron-positron pair in the collision of two real photons was first considered by Breit and Wheeler [1] who calculated the cross section for the reaction

$$\omega_1 + \omega_2 \rightarrow e^+ e^- \tag{1}$$

to be of order r_e^2, where r_e is the classical electron radius. While pair creation by real photons is believed to occur in astrophysical processes [2], it has not been observed in the laboratory up to the present.

After the invention of the laser the prospect of intense laser beams led to the reconsideration of the Breit-Wheeler process by Reiss [3] and others [4,5]. Of course, for production of an electron-positron pair, the center-of-mass (CM) energy of the scattering photons must be at least $2mc^2 \approx 1$ MeV. While this precludes pair creation by a single electromagnetic wave, the necessary CM energy can be achieved by colliding a laser beam against a high-energy photon beam created, for example, by backscattering the laser beam off a high-energy electron beam. With laser light of wavelength 527 nm (energy 2.35 eV), a photon of energy 111 GeV would be required for reaction (1) to proceed. However, with an electron beam of energy 46.6 GeV, as available at the Stanford Linear Accelerator Center (SLAC), the maximum Compton-backscattered photon energy from a 527 nm laser is only 29.2 GeV.

In strong electromagnetic fields the interaction need not be limited to initial states with two photons [3], but rather the number of interacting photons becomes large as the dimensionless, invariant parameter $\eta = e\sqrt{\langle A_\mu A^\mu \rangle}/mc^2 = e\mathcal{E}_{\rm rms}/m\omega_0 c = e\mathcal{E}_{\rm rms}\lambda_0/mc^2$

approaches or exceeds unity. Here the laser beam has laboratory frequency ω_0, reduced wavelength λ_0, root-mean-square electric field $\mathcal{E}_{\rm rms}$, and four-vector potential A_μ; e and m are the charge and mass of the electron, respectively, and c is the speed of light.

For photons of wavelength 527 nm a value of $\eta = 1$ corresponds to laboratory field strength of $\mathcal{E}_{\rm lab} = 6 \times 10^{10}$ V/cm and intensity $I = 10^{19}$ W/cm². Such intensities are now practical in tabletop laser systems based on chirped-pulse amplification [6].

Then the multiphoton Breit-Wheeler reaction

$$\omega + n\omega_0 \rightarrow e^+ e^- \tag{2}$$

becomes accessible for $n \geq 4$ laser photons of wavelength 527 nm colliding with a photon of energy 29 GeV. Similarly, the trident process

$$e + n\omega_0 \rightarrow e' e^+ e^- \tag{3}$$

requires at least five 527 nm laser photons colliding with an electron of 46.6 GeV. Reaction (3) is a variant of the Bethe-Heitler process [7] in which an $e^+ e^-$ pair is created by the interaction of a real photon with a virtual photon from the field of a charged particle.

When an electromagnetic field with four-tensor $F_{\mu\nu}$ is probed by a particle of four-momentum p_μ, an invariant measure of the strength of vacuum-polarization effects is $\kappa = \sqrt{\langle (F_{\mu\nu} p^\nu)^2 \rangle}/(mc^2 \mathcal{E}_{\rm crit})$, where $\mathcal{E}_{\rm crit} = m^2 c^3/e\hbar = mc^2/e\lambda_C = 1.3 \times 10^{16}$ V/cm is the quantum electrodynamic (QED) critical field strength [8,9] at which the energy gain of an electron accelerating over a Compton wavelength λ_C is its rest energy, and at which a

static electric field would spontaneously break down into electron-positron pairs. Indeed, the predicted rates [3–5] for reaction (2) become large only when κ approaches unity, and not necessarily when η becomes large.

When a photon of energy $\hbar\omega$ collides head-on with a wave of laboratory field strength $\mathcal{E}_{\rm rms}$ and invariant strength η, the invariant $\kappa = (2\hbar\omega/mc^2)(\mathcal{E}_{\rm rms}/\mathcal{E}_{\rm crit}) = (2\hbar\omega/mc^2)(\lambda_C/\lambda_0)\eta$ may be large. For example, in a head-on collision of a photon of energy 29 GeV with a 527 nm laser pulse ($\lambda_0 = 84$ nm), $\kappa = 0.52\eta$.

Likewise, in reaction (3), or other e-laser interactions involving vacuum polarization, the relevant invariant is $\Upsilon = \mathcal{E}^\star/\mathcal{E}_{\rm crit}$, where $\mathcal{E}^\star = 2\gamma\mathcal{E}_{\rm rms}$ is the laser field strength as viewed in the rest frame of an electron beam with laboratory energy E and Lorentz factor $\gamma = E/mc^2$. For a 46.6 GeV electron beam colliding head-on with a 527 nm laser, $\Upsilon = 0.84\eta$.

We have performed an experimental study of strong-field QED in the collision of a 46.6 GeV electron beam, the Final Focus Test Beam (FFTB) at SLAC [10], with terawatt pulses from a frequency doubled Nd:glass laser with a repetition rate of 0.5 Hz achieved by a final laser amplifier with slab geometry [11–14]. A schematic diagram of the experiment is shown in Fig. 1. The apparatus was designed to detect electrons that undergo nonlinear Compton scattering,

$$e + n\omega_0 \rightarrow e' + \omega, \tag{4}$$

as well as positrons produced in e-laser interactions. Measurements of reaction (4) have been reported elsewhere [11,15].

The peak focused laser intensity was obtained for linearly polarized green (527 nm) pulses of energy $U = 650$ mJ, focal area $A \equiv 2\pi\sigma_x\sigma_y = 30\ \mu{\rm m}^2$, and width $\Delta t = 1.6$ ps (FWHM), for which $I = U/A\Delta t \approx 1.3 \times 10^{18}$ W/cm^2, $\eta = 0.36$, $\kappa = 0.2$, and $\Upsilon = 0.3$.

The electron beam was operated at 10–30 Hz and was tuned to a focus with $\sigma_x = 25\ \mu$m and $\sigma_y = 40\ \mu$m at the laser-electron interaction point. Typical bunches were 7 ps long (FWHM) and contained 7×10^9 electrons.

A string of permanent magnets after the collision point deflected the electron beam downwards by 20 mrad. Electrons and positrons of momenta less than 20 GeV were deflected by the magnets into two Si-W calorimeters (ECAL and PCAL) with energy resolution $\sigma_E/E \approx 19\%/\sqrt{E[{\rm GeV}]}$ and position resolution of 2 mm. The Si-W calorimeters were calibrated in parasitic running of the
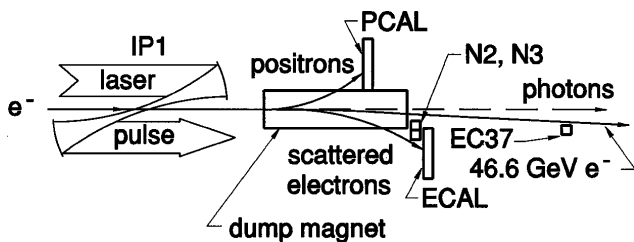
FFTB in which linac-halo electrons of energies between 5 and 25 GeV were transmitted by the FFTB when the latter was tuned to a lower energy.

Electrons scattered via reaction (4) for $n = 1$, 2, and 3 laser photons were measured in gas Čerenkov counters labeled EC37, N2, and N3 in Fig. 1. We used detectors based on Čerenkov radiation because of their insensitivity to major sources of low-energy background. EC37 was calibrated by inserting a thin foil in the electron beam at IP1. The momentum acceptance and efficiency of the counters N2 and N3 were measured with the parasitic electron beam by comparison with the previously calibrated ECAL.

The spatial and temporal overlap of the electron and laser beams was optimized by observing the Compton scattering rate of up to 10^7/pulse in the EC37, N2, N3, and ECAL detectors during horizontal, vertical, and time scans of one beam across the other.

We used the PCAL calorimeter to search for positrons produced at IP1. Because of the high rate of electrons in the ECAL calorimeter from Compton scattering, it was not possible to identify the electron partners of the positrons.

The response of PCAL to positrons originating at IP1 was studied by inserting a wire into the electron beam at IP1 to produce e^+e^- pairs by Bethe-Heitler conversion of bremsstrahlung photons. These data were used to develop an algorithm to group contiguous PCAL cells containing energy deposits into "clusters" representing positron candidates. The clusters were characterized by their positions in the horizontal ($X_{\rm pos}$) and vertical ($Y_{\rm pos}$) direction and by their total energy deposit $E_{\rm clu}$. Using the field maps of the magnets downstream of IP1, the vertical impact position was translated into the corresponding momentum $P_{\rm clu}$. Figure 2 shows the density of clusters produced by the wire in the two planes $E_{\rm clu}/P_{\rm clu}$ vs $Y_{\rm pos}$ and $Y_{\rm pos}$ vs $X_{\rm pos}$. Only clusters within the signal regions bounded by solid lines in Fig. 2 were counted as positron candidates. The efficiency of the cluster-finding algorithm is estimated to be $93 \pm 1\%$.
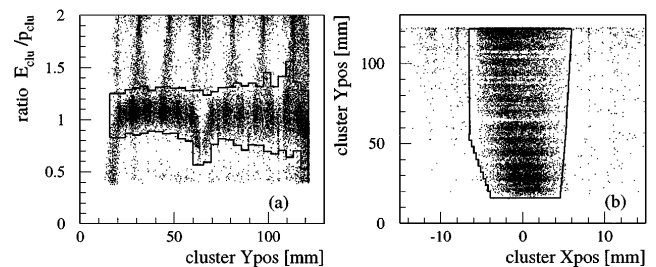

FIG. 2. Cluster densities from positrons produced by a wire inserted at IP1. The solid line shows the signal region for positron candidates. (a) Ratio of cluster energy to momentum vs vertical impact position above the lower edge of PCAL. The banding in $Y_{\rm pos}$ is an artifact of the segmentation of the detector. Two simultaneous showers separated by less than a cell caused the clusters with $E_{\rm clu}/P_{\rm clu} \sim 2$. (b) Cluster position in PCAL.

FIG. 1. Schematic layout of the experiment.

We collected data at various laser intensities. The data from collisions with poor e-laser beam overlap were discarded when the signal in the EC37 monitor was less than one-third of the expected value. The number of positron candidates observed in the remaining 21 962 laser shots is 175 ± 13 and is shown as the upper distribution in Fig. 3(a) as a function of cluster momentum.

Positrons were also produced in showers of lost electrons upstream of the PCAL detector. The rate of these background positrons was studied in 121 216 electron-beam pulses when the laser was off, yielding a total of 379 ± 19 positron candidates. Figure 3(a) shows the momentum spectrum of these candidates as the hatched distribution, which has been scaled by 0.181, this being the ratio of the number of laser-on to laser-off pulses. After subtracting the laser-off distribution from the laser-on distribution, we obtain the signal spectrum shown in Fig. 3(b) whose integral is 106 ± 14 positrons.

We have modeled the pair production as the two-step process of reaction (4) followed by reaction (2), using the formalism of Ref. [4] for linearly polarized light. The high-energy photon is linearly polarized since the laser is linearly polarized [16]. By numerical integration over space and time in the e-laser interaction region we account for both the production of the high-energy photon (through a single or multiphoton interaction) and its subsequent multiphoton interaction within the same laser focus to produce the pair. Further Compton scatters of the positron (or electron) are also taken into account. The positron spectrum predicted by this calculation is shown as the curve in Fig. 3(b) and is in reasonable agreement with the data.

To determine the effective intensity of each laser shot, i.e., the peak intensity of the part of the laser beam that overlapped with the electron beam, we made use of N_1, N_2, and N_3, the number of electrons intercepted by the gas

Čerenkov counters EC37, N2, and N3, of first-, second-, and third-order Compton scattering, respectively. Ideally, the field intensity could be extracted from each of these monitors. However, because of e-laser timing jitter [13], the effective intensity has been extracted from ratios of the monitor rates. For $\eta^2 \ll 1$, the field intensity is approximately given by $\eta^2 = k_1 N_2/N_1$ as well as $\eta^2 = k_2 N_3/N_2$. The parameters k_1 and k_2 depend on the acceptance and efficiency of the counters, as well as the spectrum of scattered electrons, and were calculated over the relevant range of η^2 in the numerical simulation. We fit the observed N_i for each event to ideal values subject to the constraint $N_2^2 = (k_2/k_1)N_1 N_3$. Then the fitted N_i determined η with an average precision of 11%. Uncertainties in the acceptance, background levels, calibration, and efficiency of the monitors caused a systematic error of $^{+8}_{-13}\%$ to the absolute value of η.

Figure 4 shows the yield (R_{e^+}) of positrons/laser shot as a function of η. The line is a power law fit to the data and gives $R_{e^+} \propto \eta^{2n}$ with $n = 5.1 \pm 0.2(\text{stat})^{+0.5}_{-0.8}(\text{syst})$, where the statistical error is from the fit and the systematic error includes the effects discussed previously, as well as the effect of the choice of bin size in η. Thus, the observed positron production rate is highly nonlinear, varying as the fifth power of the laser intensity. This is in good agreement with the fact that the rate of multiphoton reactions involving n laser photons is proportional to η^{2n} (for $\eta^2 \ll 1$), and with the kinematic requirement that five photons are needed to produce a pair near threshold. The detailed simulation indicates that, on average, 1.5 photons are absorbed from the laser field in reaction (4) and 4.7 in (2), but that the exponent n for the two-step process varies slightly with η and has an average value of 5.3.
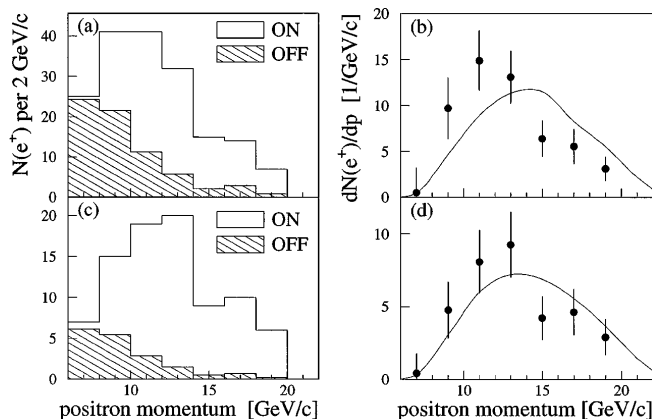

FIG. 3. (a) Number of positron candidates vs momentum for laser-on pulses and for laser-off pulses scaled to the number of laser-on pulses. (b) Spectrum of signal positrons obtained by subtracting the laser-off from the laser-on distribution. The curve shows the expected momentum spectrum from the model calculation. (c),(d) Same as (a) and (b) but with the requirement that $\eta > 0.216$.
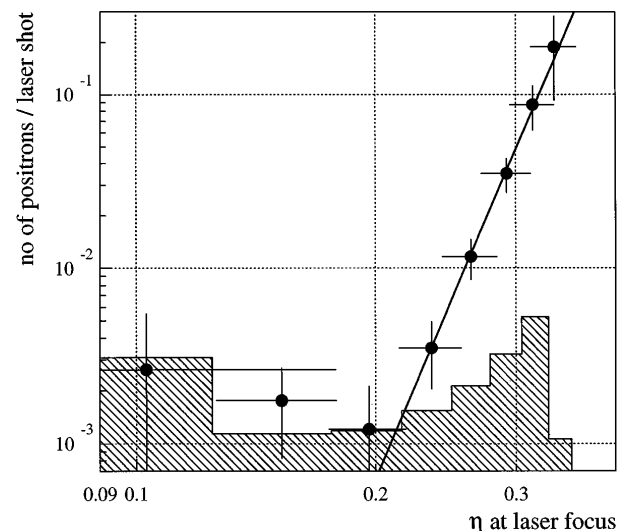

FIG. 4. Dependence of the positron rate per laser shot on the laser field-strength parameter η. The line shows a power law fit to the data. The shaded distribution is the 95% confidence limit on the residual background from showers of lost beam particles after subtracting the laser-off positron rate.

Several points at low values of η seen in Fig. 4, while statistically consistent with reactions (4) and (2), indicate a possible residual background of about 2×10^{-3} positrons/laser shot due to showers of lost beam electrons. If we restrict the data to events with $\eta > 0.216$ we find 69 ± 9 positrons, and the agreement of their momentum spectrum with the model calculation is improved, as shown in Fig. 3(d).

The observed positron rate is shown in Fig. 5 after being normalized to the number of Compton scatters, where the latter is inferred from the measured rate in the EC37 monitor. This procedure minimizes the effect of the uncertainty in the laser focal volume and in the e-laser overlap. The simulation indicates that the variation of the positron rate over a spatial offset of ± 25 μm, or a temporal offset of ± 5 ps between the electron and laser beams, is 0.88 ± 0.07 of the variation in the Compton scattering rate. The solid curve in Fig. 5 shows the prediction based on the numerical integration of the two-step Breit-Wheeler process, (4) followed by (2), multiplied by the cluster-finding efficiency (0.93) and the overlap correction factor (0.88). The data are in good agreement with the simulation, both in magnitude of the observed rate and in its dependence on η.

Although we have demonstrated a signal of positron production associated with the scattering of laser light, we cannot immediately distinguish positrons from reaction (2) from those originating in the trident process (3). A complete theory of reaction (3) does not exist at present so we performed a simulation based on a two-step model in which the beam electron emits a virtual photon according to the Weizsäcker-Williams approximation, and
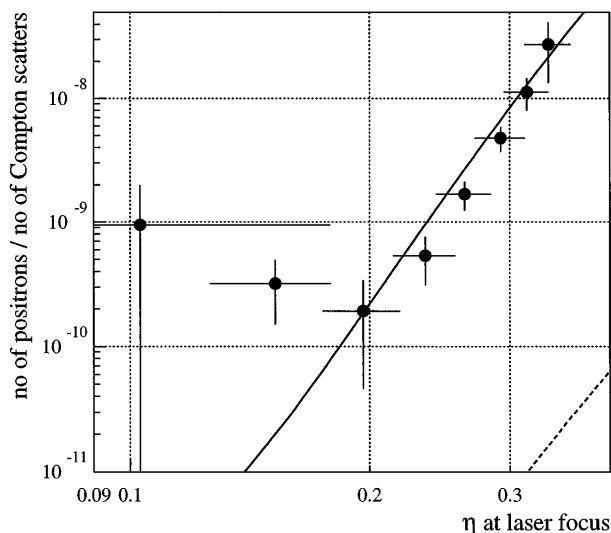
the virtual photon combines with laser photons to yield electron-positron pairs according to the theory of the multiphoton Breit-Wheeler process (2). The results of this simulation indicate that for the present experiment the trident process is negligible, as shown in Fig. 5 by the dashed line.

These results, as well as those of Ref. [15], confirm the validity of the formalism of strong-field QED and show that the observed rates for the multiphoton reactions (2) and (4) are in agreement with the predicted values. Furthermore, these results are the first observation of inelastic photon-photon scattering with real photons.

FIG. 5. Dependence of the positron rate on the laser field-strength parameter η when the rate is normalized to the number of Compton scatters inferred from the EC37 monitor. The solid line is the prediction based on the numerical integration of the two-step Breit-Wheeler process, (4) followed by (2). The dashed line represents the simulation for the one-step trident process (3).

*Present address: Hughes Leitz Optical Technologies Ltd., Midland, Ontario, Canada L4R 2H2.
†Present address: Lawrence Livermore National Laboratory, Livermore, California 94551.
‡Present address: Stanford Linear Accelerator Center, Stanford University, Stanford, California 94309.
§Also at Department of Mechanical Engineering.
‖Present address: Panoramastrasse 8, 78589 Durbheim, Germany.

[1] G. Breit and J. A. Wheeler, Phys. Rev. **46**, 1087 (1934).
[2] O. C. De Jager *et al.,* Nature (London) **369**, 294 (1994).
[3] H. R. Reiss, J. Math. Phys. **3**, 59 (1962).
[4] A. I. Nikishov and V. I. Ritus, Sov. Phys. JETP **19**, 529 (1964); **19**, 1191 (1964); **20**, 757 (1965); **25**, 1135 (1967).
[5] N. B. Narozhny *et al.,* Sov. Phys. JETP **20**, 622 (1965).
[6] D. Strickland and G. Mourou, Opt. Commun. **55**, 447 (1985).
[7] H. A. Bethe and W. Heitler, Proc. R. Soc. London A **146**, 83 (1934).
[8] F. Sauter, Z. Phys. **69**, 742 (1931).
[9] W. Heisenberg and H. Euler, Z. Phys. **98**, 718 (1936).
[10] V. Balakin *et al.,* Phys. Rev. Lett. **74**, 2479 (1995).
[11] T. Kotseroglou, Ph.D. thesis, University of Rochester, 1996 (unpublished).
[12] S. J. Boege, Ph.D. thesis, University of Rochester, 1996 (unpublished).
[13] T. Kotseroglou *et al.,* Nucl. Instrum. Methods Phys. Res., Sect. A **383**, 309 (1996).
[14] C. Bamber *et al.,* Laser Phys. **7**, 135 (1997).
[15] C. Bula *et al.,* Phys. Rev. Lett. **76**, 3116 (1996).
[16] U. Fano, J. Opt. Soc. **39**, 859 (1949).